Supporting Information for

Chemical Speciation of Nanoparticles Surrounding Metal-on-Metal Hips

Angela E Goode[a], James M Perkins[a], Ann Sandison[b], Chithra Karunakaran[c], Huikai Cheng[d], David Wall[d], John Skinner[e], Alister J Hart[f], Alexandra E Porter[a*], David W McComb[a,g*] and Mary P Ryan[a*]

[a]Department of Materials, Imperial College London, London, UK

[b] Department of Orthopaedics, Royal National Orthopaedic Hospital, UK

[c] Canadian Light Source, Saskatoon, Canada

[d]FEI Company, The Netherlands and USA

[e]Centre for Clinical Orthopaedics, University College London, London, UK

[f] Charing Cross Hospital, Imperial College London, London, UK

[g] Department of Materials Science & Engineering, The Ohio State University, USA

*corresponding author

Detailed Methods

Sample preparation. Hip capsule tissue was analysed from 3 patients with a failed MOM hip resurfacing arthroplasty. Blood levels of cobalt and chromium were measured by inductively coupled plasma mass spectrometry (ICP-MS). For histological analysis, samples of hip capsule were fixed in 10% neutral buffered formalin, and selected blocks were processed to paraffin wax. 3-4 μm thick sections were cut and stained with haematoylin and eosin using routine methods. For TEM and XAS studies, tissue was fixed in 3% glutaraldehyde in and cacodylate buffer, post-fixed in 1% osmium tetroxide, dehydrated through a graded series of ethanol and embedded in Araldite epoxy resin. An ultramicrotome with 35° diamond knife was used to cut 150 nm thick sections, which were collected onto standard copper TEM grids.

Locating wear debris. Sections from these 3 patients were examined using the JEOL 2000FX TEM at 120 kV, under bright field imaging conditions. Electron-dense particles of the right length scale (~50 nm) were further examined using an INCAx-sight EDX detector to determine their chemical composition. These data were published in Ref 16 and will not be discussed in detail here: briefly they showed high concentrations of Cr and a significantly reduced concentration of Co in the host

tissue for all patients. One of these patients was selected for further detailed analysis with EELS and STXM. Slice and View was carried out on a 6 µm × 6 µm × 8 µm volume of embedded tissue using an FEI Helios Nanolab with fully automated program Slice and View™. 10 nm slices were milled with a 30 keV ion beam and the surfaces were imaged with a 2 keV beam using in backscattered electron using the in-lens detector mode. Volume reconstruction was performed using Amira 3D visualisation software (Mercury Computer Systems, France). Analysis of particle sizes was performed using ImageJ software. Quantitative analysis of the size and morphology of particulate debris was performed using ImageJ software by employing a thresholding procedure to identify the particles.

Scanning Transmission X-ray Microscopy – X-ray Absorption Spectroscopy (STXM-XAS). STXM experiments were carried out at beamline 10ID-1 at the Canadian Light Source (CLS). Sections which had been mapped in the TEM, so areas of high particle concentration could be located quickly. Serial sections, which had not been previously exposed to the electron beam, were also analysed. The X-ray probe size was 25 nm and the spectra were recorded in transmission mode. Areas of approximately 10 µm × 10 µm were analysed by taking 'stacks' over the oxygen K-edge and chromium and cobalt $L_{2,3}$-edges. This involved acquiring sets of X-ray absorption images at a range of different photon energies. XAS spectra of the following reference compounds were also acquired: Cr_2O_3, $K_2Cr_2O_7$, $CrPO_4$, $(AcO)_7Cr_3(OH)_2$ and CoO. Data processing was performed using stack_analyze [1], pca_gui [2] and aXis2000 [3] software. Transmitted flux was normalised against the incident flux and images were aligned using cross-correlation to compensate for the lateral movement of the zone plate and thermal drift. Distribution maps of the components in the sample were calculated using two techniques, singular value decomposition and principal component analysis (not shown).

Scanning Transmission Electron Microscopy - Electron Energy Loss Spectroscopy (STEM-EELS) and Energy Dispersive X-ray analysis (STEM-EDX). Sections analysed by STXM were subsequently examined in the FEI Titan (S)TEM at 300 kV. Bright field images in TEM mode, as well as high angle annular dark field (HAADF) images in STEM mode, were acquired. EELS spectra were recorded on a GIF Tridiem spectrometer with a dispersion of 0.2 eV per channel. The convergence and collection semi-angles were 7 mrad and as 18 mrad respectively, and the energy resolution was 0.7 eV. EELS data were acquired as 'spectrum images', in which the electron beam is rastered over the sample and a complete EELS spectrum was acquired at each probe position. Spectra were processed using DigitalMicrograph™ (DM) software. Background of the form AE^{-r} was subtracted from each edge individually, and spectra were deconvolved to remove plural scattering. As the Cr L edge lies close to the O K edge, a linear regression fit of the oxygen signal

was calculated in DM and subsequently removed using an *ad hoc* MATLAB script. Quantification was carried out in DM to calculate the numbers of oxygen, chromium and cobalt atoms in each nm^2 of sample (nominally 150 nm thick) using the equation:

$$I_k(\Delta) = N\sigma_k(\Delta)I(\Delta) \quad (1)$$

where N is the areal concentration (atoms / nm^2) of the atoms giving rise to the ionization edge k, I_k is the integrated intensity of the edge (using a 40 eV window), I is the integrated intensity of the low loss region including the zero-loss peak (40 eV window), and σ_k is the partial inelastic scattering cross-section. Cross-sections were calculated using the Hartree-Slater model for the oxygen K edge and the 'hydrogenic white line' model for the metal L edges.

STEM-EDX experiments were performed in a Tecnai Osiris (S)TEM microscope operated at 200 kV, with a probe current of 0.3 nA and nominal probe size of 0.3 nm. EDX maps were obtained over areas of ~4.5 × 3.5 μm, using pixel sizes of 5 nm and dwell times of 50 μs per pixel.

References

1. Jacobsen, C.; Wirick, S.; Flynn, G.; Zimba, C. *J Microsc.* **2000,** 197, 173-84.
2. Lerotic, M.; Jacobsen, C.; Schafer, T.; Vogt, S. *Ultramicroscopy* **2004,** 100, 35-57.
3. *aXis2000 is written in Interactive Data Language (IDL), and is available from http://unicorn.mcmaster.ca/aXis2000.html.*

Supplementary Figures

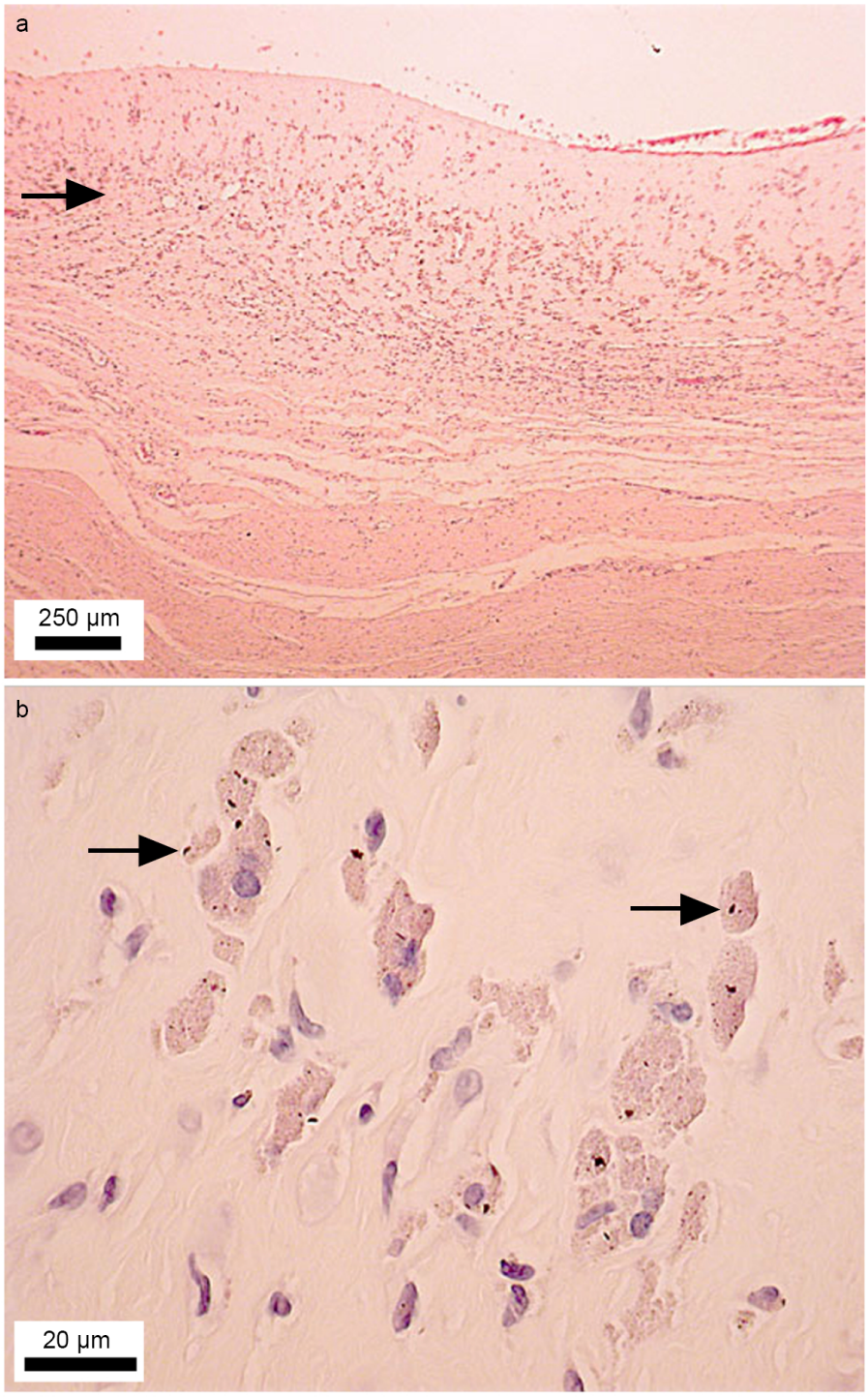

Figure SI1. Cross section of the capsular surface adjacent to the synovial cavity imaged with light microscopy. (a) Ultramicrotomed sections show an inflammatory response in the tissue, and a subsurface band of macrophage cells is visible (arrow) (b) Higher magnification image of macrophage cells within this band reveals the presence of dark regions (arrows) in the cytoplasm thought to be wear debris.

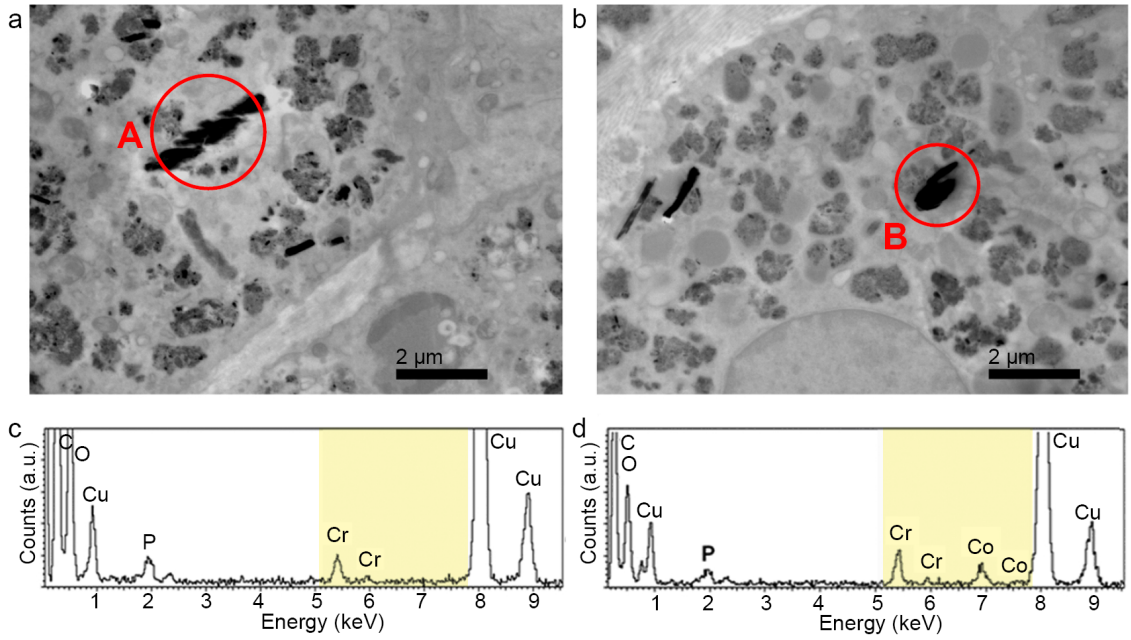

Figure SI2. (a-b) Bright field TEM images showing electron dense debris (dark particles) clustered in the cytoplasm of macrophage cells. (c-d) EDX analysis of circled particles shows that particle A contains Cr while particle B contains both Cr and Co. The Cu signal originates from the TEM grid on which the section is supported.

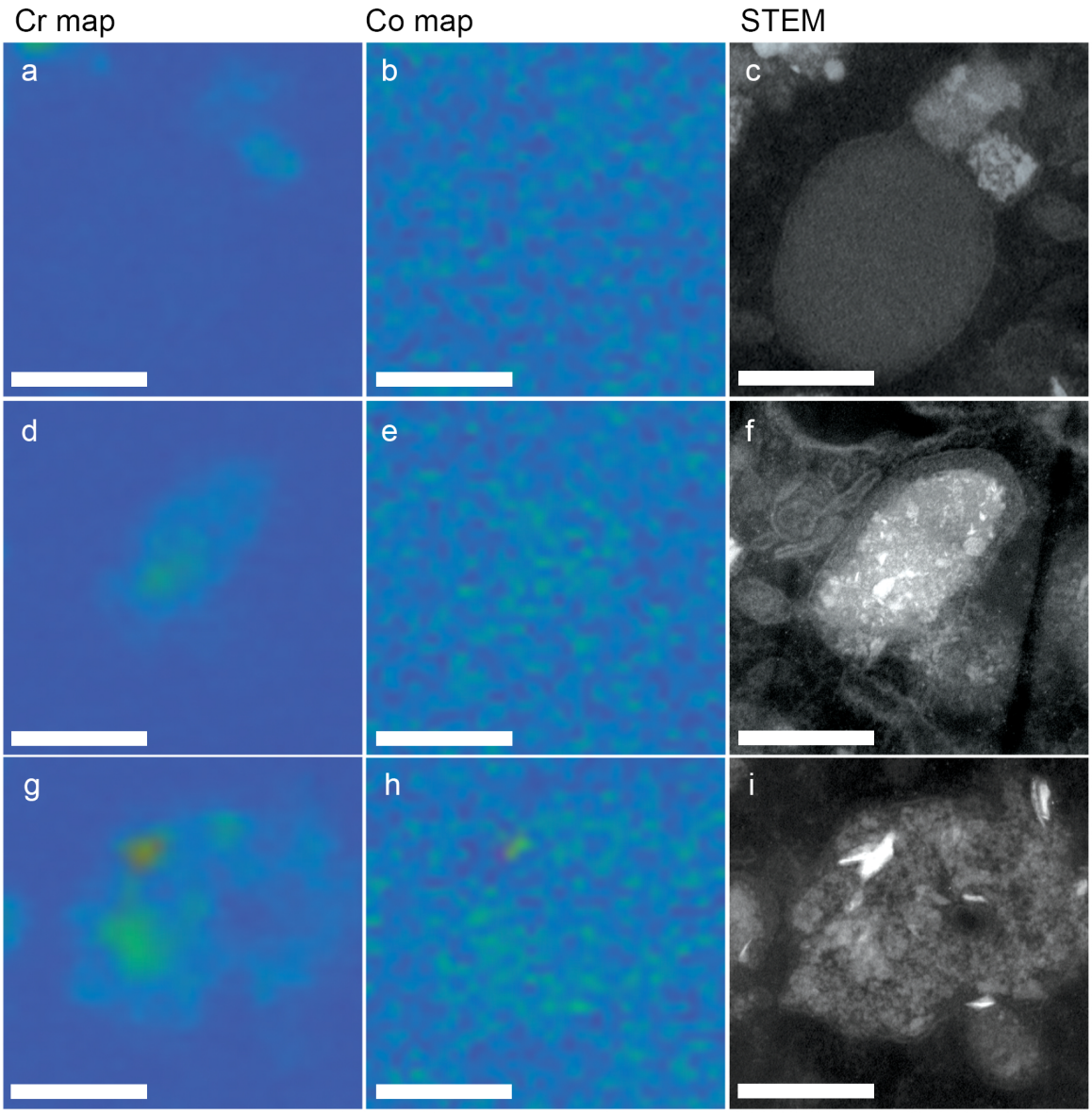

Figure SI3. Different clusters of wear debris analysed by STXM and dark field STEM. Cr (a,d,g,j) and Co (b,e,h,k) chemical thickness maps and dark field STEM images (c,f,i,l) of wear debris clusters are correlated. (scale bars 400 nm)

SI4. Video showing the 3D reconstruction of a volume within a macrophage cell.

The series of SEM images obtained by slice and view in the dual beam FIB is displayed as well as a voltex rendering of a smaller volume within this dataset. Here, wear debris is visualised as green particles and the diffuse blue spheres correspond to lipid droplets. A number of the larger wear particles (yellow) are shown separately so that their morphology is more clearly displayed.